

# Cosmological Origin of the Lowest Metallicity Halo Stars

Xavier Hernandez<sup>1</sup> and Andrea Ferrara<sup>1,2</sup>

<sup>1</sup> *Osservatorio Astrofisico di Arcetri, Largo E. Fermi 5, 50125 Firenze, Italy*

<sup>2</sup> *Center for Computational Physics, University of Tsukuba, Tsukuba-shi, Ibaraki-ken, 305-8577, Japan*

27 October 2018

## ABSTRACT

We explore the predictions of the standard hierarchical clustering scenario of galaxy formation, regarding the numbers and metallicities of PopIII stars likely to be found within our Galaxy today. By PopIII we shall be referring to stars formed at large redshift ( $z > 4$ ), with low metallicities ( $[Z/Z_{\odot}] < -2.5$ ) and in small systems (total mass  $\lesssim 2 \times 10^8 M_{\odot}$ ) that are extremely sensitive to stellar feedback, and which through a prescribed merging history (Lacey & Cole 1993) end up becoming part of the Milky Way today. An analytic, extended Press-Schechter formalism is used to get the mass functions of halos which will host PopIII stars at a given redshift, and which will end up in Milky Way sized systems today. Each of these is modeled as a mini galaxy, with a detailed treatment of the dark halo structure, angular momentum distribution, final gas temperature and disk instabilities, all of which determine the fraction of the baryons which are subject to star formation. Use of new primordial metallicity stellar evolutionary models allows us to trace the history of the stars formed, give accurate estimates of their expected numbers today, and their location in  $L/L_{\odot}$  vs.  $T/K$  HR diagrams. A first comparison with observational data suggests that the IMF of the first stars was increasingly high mass weighted towards high redshifts, levelling off at  $z \gtrsim 9$  at a characteristic stellar mass scale  $m_s = 10 - 15 M_{\odot}$ .

**Key words:** galaxies: formation – galaxies: evolution – Galaxy: formation – Galaxy: abundances – stars: luminosity function, mass function

## 1 INTRODUCTION

The formation and the properties of the first stars in the universe are probably among the most fascinating problems in present-day cosmology. Numerical simulations and analytical studies in a cosmological context (Tegmark *et al.* 1997, Abel *et al.* 1998, Bromm, Coppi & Larson 2000, Machacek, Bryan & Abel 2000) have reached a consensus on the fact that the fragments potentially leading to star formation were already available inside very small dark matter halos at redshift  $z \approx 30$  in most cosmological models. After that point the requirements concerning the dynamic range and number of physical processes to be treated become so demanding that one has to turn to simplified and/or lower dimensional studies. Although considerably refined, these studies (Omukai & Nishi 1999, Susa & Umemura 2000, Nakamura & Umemura 2000, Ripamonti *et al.* 2000) have not yet reached an agreement on the mass of the stellar seed (core) and on the accretion rate by which the former grows into a star. Determining if and when the accretion is quenched seems to hold the key for the understanding of the properties of the first stars. However, the large variety of physical effects to be

considered (for a review see Ferrara 2000) again complicate the problem tremendously.

On general grounds some authors have speculated that the IMF of the first stars can be skewed towards high stellar masses (Larson 1998) or even be bimodal (Nakamura & Umemura 2000). One of the consequences of this assumption is an increase of the relative number of massive, short-lived stars. These stars will soon end their life as supernovae, leaving either a compact remnant (a neutron star or a black hole) or nothing at all (for masses above  $\approx 120 M_{\odot}$ , see Umeda *et al.* 2000 and Fryer, Woosley & Heger 2000), and possibly releasing detectable bursts of gravitational waves (Schneider *et al.* 2000). In turn, this implies a strong decrease of the amount of zero- or very low-metallicity stars presumably included in the present-day Milky Way (MW), according to the hierarchical paradigm. Given the above discussion it appears that number counts of very low-metallicity MW stars can not only provide evidences for “living fossils”, *i.e.* stars formed immediately after the end of Dark Ages, but also probe the primordial IMF and hierarchical models to cosmic epochs ( $z \gtrsim 6$ ) currently unreachable to essentially all experiments.

We propose here that the first stars are born inside the so-called PopIII objects (Haiman & Loeb 1996, Gnedin & Ostriker 1997, Ciardi *et al.* 2000) *i.e.* systems with total mass  $\lesssim 2 \times 10^8 M_\odot$ , which strongly rely on molecular hydrogen cooling in order to collapse, given their low virial temperatures; in short, we define as PopIII stars those formed inside such mini galaxies. As Ciardi *et al.* have pointed out, these objects are extremely fragile to the energy release by their own supernovae; as a result, their gas is quickly evacuated and they can only witness a single burst of star formation. The remnant is a "naked stellar object" (Ciardi *et al.* 2000), *i.e.* a tiny agglomerate of long lived low-mass stars, essentially retaining the metallicity of the gas from which they formed. These are the stars that we are considering as candidates for the very low-metallicity stars observed in the MW halo.

Our paper is structured as follows: the next section presents the Press-Schechter formalism used to calculate the mass functions of MW sub-galactic clumps at different redshifts. In Section 3 we describe the treatment of PopIII halos as mini galaxies to estimate the number of stars each contributes to the final MW. Section 4 gives a comparison with recent observational results of the numbers and metallicity distribution of extremely low metallicity halo stars. Finally, a brief summary is given in Section 5.

## 2 BUILD UP OF THE MILKY WAY

We use the extended Press-Schechter formalism to calculate the conditional probability that a virialized halo of mass  $M_1$  at  $z_1$  will become part of a more massive halo of mass  $M_0$  at a later time,  $z_0$ . This allows us to calculate the mass functions of the fragments which through mergers will end up as part of a MW sized system today. Following Nusser & Sheth (1999), we identify the mass contained in progenitors of mass between  $M_1$  and  $(M_1 + dM_1)$  with:

$$\Delta M = \frac{M_0}{\sqrt{2\pi}} \frac{\delta_c(z_1 - z_0)}{(S_1 - S_0)^{3/2}} \exp \left[ -\frac{\delta_c^2(z_1 - z_0)^2}{2(S_1 - S_0)} \right] \left| \frac{dS_1}{dM_1} \right| dM_1 \quad (1)$$

In the above expression  $\sqrt{S_i}$  is the rms density fluctuation in a top hat window function of radius  $(3M_i/4\pi\rho_0)^{1/3}$ , and  $\delta_c$  the critical overdensity for collapse, with  $\rho_0 = 3\Omega_M H_0^2/8\pi G$  being the present mean mass density of the universe. Both of the above quantities were calculated using a  $\Lambda$ CDM power spectrum normalized to  $\sigma_8 = 0.91$ , in a  $\Omega_\Lambda = 0.7$  flat universe ( $\Omega_M = 0.3$ ), with  $H_0 = 65 \text{ km s}^{-1} \text{ Mpc}^{-1}$ , which we used throughout, *e.g.* Percival & Miller (1999). A baryonic fraction of 0.05 of the total halo mass was assumed for all halos.

Current direct estimates of the mass of the MW rely on distant galactic satellites used as probes of the mass internal to their current positions, using their line of sight velocities and reasonable assumptions on their orbits. These methods give values for the total mass of the MW of around  $1 \times 10^{12} M_\odot$ , *e.g.* Kulessa & Lynden-Bell (1992), Binney & Merrifield (1998). However, those estimates yield only lower limits, as the total extent of the Galactic dark halo could be greater than the current positions of suitably observable satellites. Consistently with the Press-Schechter approach we are using, we estimate the total mass of the MW as the

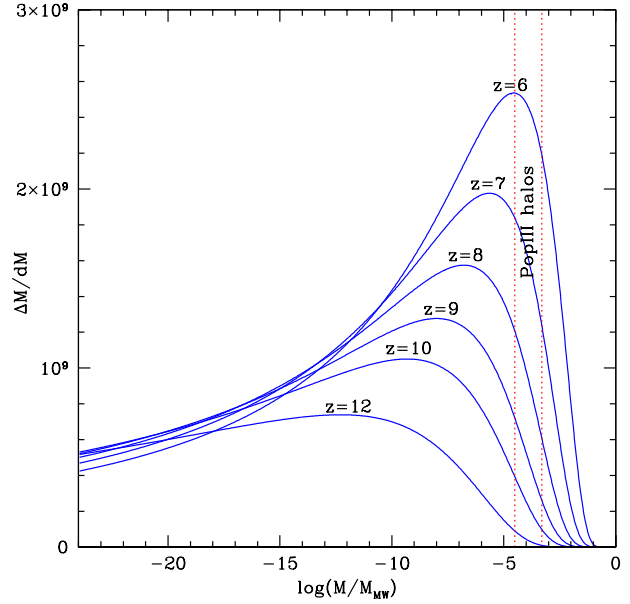


**Figure 1.** Mass functions of halos which at  $z = 0$  end up as part of a  $2 \times 10^{12} M_\odot$  system, *i.e.* similar to the MW, at different redshifts. The dotted lines indicate the mass range where PopIII stars are expected to form.

total mass contained within a sphere of radius  $r_{200}$ , the radius inside which the average density is 200 times the present background density,  $\rho_{200} = 200 \times \rho_0$ . This in fact is the only meaningful definition of “galaxy” within the Press-Schechter approach. The circular velocity at this radius would be around  $V_{max} = \sqrt{2} \times V_{200}$ , where  $V_{max} = 220 \text{ km s}^{-1}$  and the factor of  $\sqrt{2}$  between  $V_{max}$  and  $V_{200}$  is deduced from CDM simulations *e.g.* Avila-Reese *et al.* (1999), Steinmetz & Navarro (1999). This gives:

$$M_{MW} = \left( \frac{3}{4\pi} \right)^{1/2} \frac{V_{200}^3}{G^{3/2} \rho_{200}^{1/2}} \quad (2)$$

which for the adopted cosmological model gives  $2.6 \times 10^{12} M_\odot$ , somewhat above the observational lower limits. In what follows we shall use  $M_{MW} = 2.0 \times 10^{12} M_\odot$ , within the uncertainties associated with going from  $V_{max}$  to  $V_{200}$ , and in determining  $V_{max}$ .

Fig. 1 shows the mass of sub-halos which at  $z = 0$  find themselves included in MW sized halos, as a function of sub-halo mass, at different redshifts; the dotted lines show the limits within which halos at the redshifts shown will form PopIII halos.

We associate a maximum metallicity to the stars to be formed and contained within these halos through the mean mass weighted metallicity of the universe at each redshift, as calculated by Gnedin & Ostriker (1997) using fully hydrodynamic simulations. As a result of the merger process, these halos will probably contain a few stars with yet lower metallicities formed in halos of the preceding hierarchies; in this sense we take the metallicities of Gnedin & Ostriker (1997) as an upper limit for the stars of these halos.

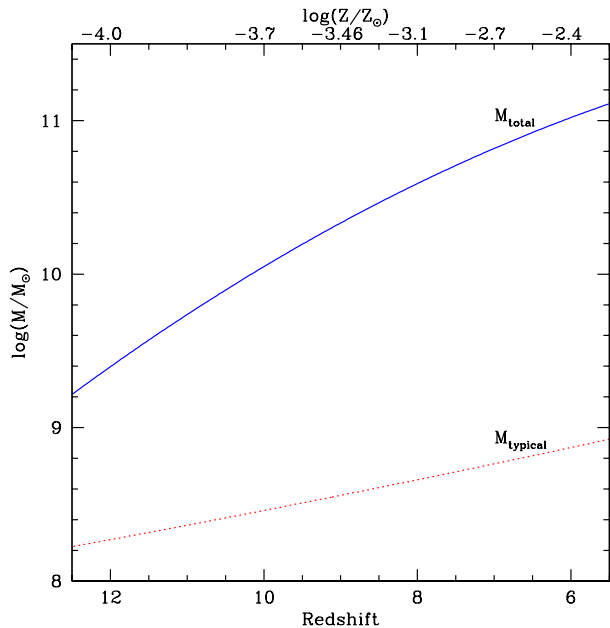


**Figure 2.** Total mass in PopIII halos that ends up in a MW sized galaxy today, as a function of redshift (solid line). The dotted curve shows the typical mass of these PopIII halos. The upper axis shows the average metallicity of the IGM at that redshift.

The lower mass limit,  $M_{crit}$ , is taken from Tegmark *et al.* (1997) (see however Fuller & Couchman 2000). Systems having virial temperatures below this curve cannot cool in a Hubble time. The upper limit,  $M_{by}$ , corresponds to the upper mass at which the stellar feedback due to supernova can expel the baryonic component entirely, thus quenching further star formation. Following Ciardi *et al.* (2000), we define this as a "blowaway", and we adopt their determination for the evolution of  $M_{by}$ . Thus, larger systems where self enrichment can continue and stars of metallicities higher than the Gnedin & Ostriker (1997) limit will be formed are excluded. However, given the sharply decreasing mass functions, our results are rather insensitive to this upper limit. These two limits change slightly with redshift, the ones shown are typical for the redshifts displayed, although the more detailed redshift dependent estimates discussed above were used.

Fig. 2 shows the integral of the PopIII halos mass functions between the selected limits,  $M_{total}$ , as a function of redshift. The upper axis shows the mean mass weighted metallicity corresponding to each redshift, discussed above. Fig. 2 also gives the typical mass of a single PopIII halo,  $M_{typical}$ , showing that within the redshift interval displayed, each present day MW sized system will have had between 10 and 100 PopIII halos as progenitors, contributing stars with metallicities in  $-4.0 < [Z/Z_{\odot}] < -2.4$ . This means that the mass functions of eq. 1 will be sampled densely, and the spread between different present day systems will be minimal i.e., all MW sized systems should contain the same numbers and distribution of stars having metallicities in the above range. The two curves of Fig. 2 intersect at a redshift of  $\sim 15$ , corresponding to a metallicity of  $[Z/Z_{\odot}] = -4.3$  in the Gnedin & Ostriker picture. At this

limit many present day MW sized systems will have had only one PopIII halo coming from beyond this redshift, and many will have had none at all. In this way we can expect that the numbers of stars in the Milky Way with metallicities below  $[Z/Z_{\odot}] = -4.3$  should be minimal, indeed, no such stars have been found to date.

For even lower metallicities, one goes to larger limiting redshifts to reach  $z \sim 30$ ,  $Z/Z_{\odot} \approx 0$  and  $M_{typical} \sim 10^6 M_{\odot}$ , the objects responsible for the appearance of the very first stars and of starting the reionization of the universe. However, as commented above, the chance of finding any such object as part of the MW is slim, they will be found as part of larger systems, perhaps as intracluster stars. For simplicity though, we will use the term first stars to identify the earliest stars of our Galaxy.

### 3 FORMING THE FIRST STARS

#### 3.1 Disk Formation

We model each of the PopIII halos discussed above as a small galactic system. Systems with masses larger than  $M_{crit}$  cool and the gas forms a disk in centrifugal equilibrium (often seen in the numerical simulations quoted above), with an exponential surface density profile fixed by the total baryonic mass and angular momentum. This last is given by the  $\lambda$  parameter, which is chosen at random from the distribution:

$$P(\lambda) = \frac{1}{\sigma_{\lambda}(2\pi)^{1/2}} \exp\left[-\frac{\ln^2(\lambda / \langle \lambda \rangle)}{2\sigma_{\lambda}^2}\right] \frac{d\lambda}{\lambda}, \quad (3)$$

with  $\langle \lambda \rangle = 0.05$  and  $\sigma_{\lambda} = 1.0$ , *e.g.* Dalcanton *et al.* (1997) and references therein. The initial dark halo profile is chosen such to have a central constant density core, as seen in present day dark halos from dwarf to cluster scales, Firmani *et al.* (2000). The formation of the disk modifies the gravitational potential in the central regions, we include the reaction on the dark halo to this process through an adiabatic invariance hypothesis (Flores *et al.* 1993; Hernandez & Gilmore 1998).

Fig. 3 shows a typical PopIII proto-galaxy, having a total mass of  $3 \times 10^8 M_{\odot}$ , with a close-to-average angular momentum,  $\lambda = 0.035$ . The final rotation curve is given by the solid curve, with the dotted line giving the surface density profile of the disk.

#### 3.2 Disk Instabilities

The final temperature of the gas in the disk is taken to be  $300K$ , as appropriate for gas where the main cooling mechanism is  $H_2$  (Ferrara 1998, Susa & Umemura 2000, Machacek *et al.* 2000). This temperature determines  $c_s$ , the sound speed within the disk, which together with  $\kappa$ , the epicycle frequency obtained from the detailed final rotation curve, yields the Toomre's stability parameter for the disk:

$$Q = \frac{c_s \kappa}{\pi G \Sigma}. \quad (4)$$

In the regions where  $Q > 1$  the total tidal shears, together with the velocity dispersion, are sufficient to stabilize the disk locally against its self gravity. These regions are therefore not subject to star formation. The dashed curve

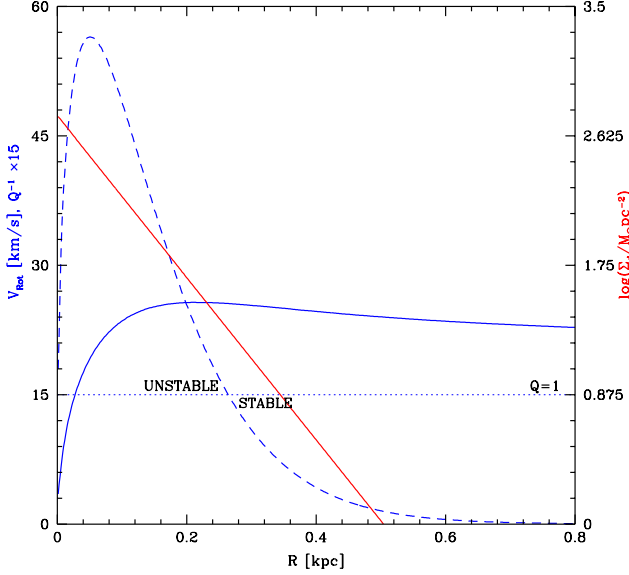


**Figure 3.** A typical PopIII galaxy, total mass  $3 \times 10^8 M_\odot$ , with a close to average angular momentum,  $\lambda = 0.035$ . The solid curve gives the rotation curve. The red line represents the baryonic disk surface density profile; together with the estimated sound speed in the disk, it gives the inverse of Toomre parameter,  $Q^{-1}$ , shown by the dashed line. The  $Q = 1$  instability threshold is shown by the dotted line, with the intersection of this and the  $Q^{-1}$  curve defining the stable and unstable regions.

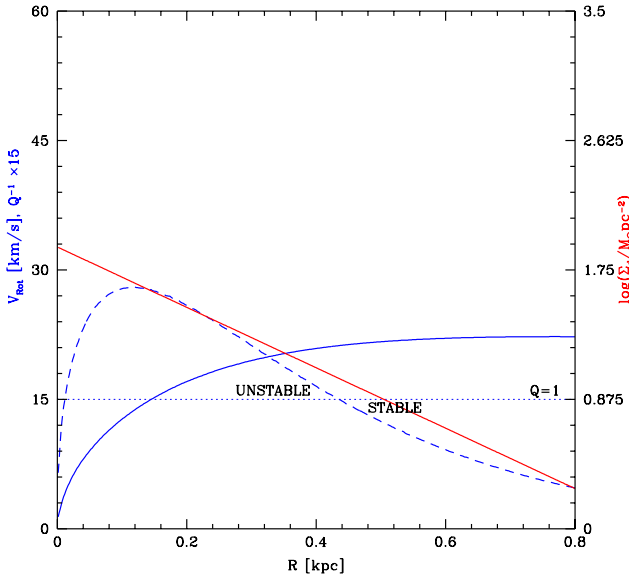


**Figure 4.** Same as Fig. 3, but for a higher value of the angular momentum,  $\lambda = 0.08$ . The changes in surface density profile, rotation curve (through the gravitational coupling of the disk and halo) and Toomre's parameter result in a larger instability radius, but a much reduced fraction being susceptible to star formation.

in Fig. 3 gives the profile of  $Q^{-1}$  in the disk, showing the regions interior to the intersection with the  $Q = 1$  line to be unstable towards star formation, in this case 85% of the disk mass. Fig. 4 is analogous to Fig. 3, but for a system having a larger angular momentum,  $\lambda = 0.08$ . The changes in disk surface density and rotation curve imply that now only a smaller fraction (60%) of the disk will form stars. A value for the gas temperature lower than the 300K we are assuming, due to the small presence of heavy elements in these objects, would only increase slightly the value of the unstable fraction. Given that the unstable fractions for systems with typical values of  $\lambda$  are already close to unity, this detail does not affect our conclusions.

Finally, a gas to star conversion efficiency  $f_* = 0.05$  is used to turn the total mass within the instability region into a final mass of stars, for each object. Although we have calibrated this parameter from local observations (Ciardi et al. 2000), since there is no firm theoretical prediction for any evolution with redshift of it, we have not explored such possibility.

### 3.3 Cloud Collisions and Collapse

Although the above instability criterion might be satisfied, it does not necessarily follow that the considered PopIII objects will be able to form stars. In fact, it is possible that cloud-cloud collisions might disrupt the gas clouds formed by the gravitational instability before they have time to collapse (a point originally made by Kashlinsky & Rees 1983). To explore this possibility we calculate the time for collisions between clouds,  $t_{coll}$  and for cloud collapse,  $t_{ff}$ . This last will be given by:

$$t_{ff} \simeq \left( \frac{1}{G\rho} \right)^{1/2}, \quad (5)$$

where  $\rho$  is the density of the gas clouds. The collisional time scale is

$$t_{coll} = (\pi \mathcal{N} \lambda_J^2 c_s)^{-1}, \quad (6)$$

with  $\mathcal{N}$  the number density of clouds, and  $\lambda_J$  the Jeans length in the disk (in general a function of radius) which we take as a representative size for the clouds. Taking  $\mathcal{N} = f_c \rho / M_J$ , where  $f_c$  is the volume fraction of the disk filled with clouds, a filling factor, and the Jeans mass

$$M_J = \left( \frac{\pi \rho}{6} \right) \left( \frac{\pi c_s^2}{G\rho} \right)^{3/2}, \quad (7)$$

since the Jeans length is:

$$\lambda_J = \left( \frac{\pi c_s^2}{G\rho} \right)^{1/2}, \quad (8)$$

we can calculate the ratio of the collision time to the collapse time by substituting the values above into eqs. 5 and 6 to yield,

$$\frac{t_{coll}}{t_{ff}} = \frac{2.9}{f_c}. \quad (9)$$

Eq. 9 shows that even if the filling factor for the fragmenting disk were unity, which is unlikely, the collapse time of the clouds is always shorter than the collision time, at all radii, and independent of the value of  $c_s$ . This is a result of having

taken a constant value of  $c_s$  throughout the disk, which is a consequence of  $H_2$  being the dominant cooling mechanism operating in the primordial metallicity gas. As eq. 9 shows, for all the scales of our problem, gravitational cloud collapse can proceed unimpeded by cloud-cloud collisions, which we shall not consider further.

### 3.4 The First Stars Today

Once the total gas mass turned into stars as a function of the metallicity has been determined, we use the IMF of Larson (1998) to turn this into a total number of stars. This function offers a convenient parameterization of the IMF:

$$dN/d\log m \propto (1 + m/m_s)^{-1.35}. \quad (10)$$

In the above equation  $m_s$  is a characteristic mass scale, of order  $0.35M_\odot$  for a present day solar neighbourhood IMF. This scale mass can be increased to explore the consequences of a top heavy IMF applying to stars of metallicities much lower than solar, as the ones we are treating.

We combine this sampling of the IMF using  $m_s = 0.35M_\odot$  with the most recent Padova stellar models of Girardi *et al.* (2000) to exclude those stars which due to their age have by now evolved off the tip of the RGB, and are hence no longer visible. In this way we obtain a sample of present day stars. Sampling the IMF from a fixed lower luminosity up to the tip of the RGB of the theoretical isochrones allows us to obtain the number of stars visible today upwards of a certain limiting luminosity, as a function of metallicity. Our final samplings include only stars between  $0.6M_\odot$  and the tip of the RGB of the Padova isochrones (of around  $1.0M_\odot$ ), which is the range over which stellar models were calculated.

As the total mass in PopIII objects is high, both the PopIII halos mass functions and the  $\lambda$  distributions are sampled densely, yielding a low spread for the predicted final number of stars.

To summarize, each of the PopIII object selected from the mass function of eq. 1 is carefully modeled as a mini galaxy, with a value of  $\lambda$  selected at random from eq. 3. The resulting system is then treated as a mini galaxy where the cooling of the baryons leads to disk formation; subsequently a disk instability criterion is used to obtain the total mass in stars contributed by each object. Finally, through the use of an IMF and new low metallicity stellar models, this total mass is turned into a number of stars visible today. This is repeated until the total PopIII object mass equals that within the bounded region described in Section 2, for a given limiting redshift, which corresponds to a fixed maximum metallicity. This process is repeated for different limiting redshifts, to construct a total mass distribution function for the low metallicity stars for the present day MW. The curve in Fig. 5 shows the number of MW stars with mass in the above range and having metallicities lower than a given value.

## 4 COMPARISON WITH DATA

To compare our results with observations we take the sample of Ryan & Norris (1991) of low metallicity halo stars in the local disk. They include a magnitude limited sample,

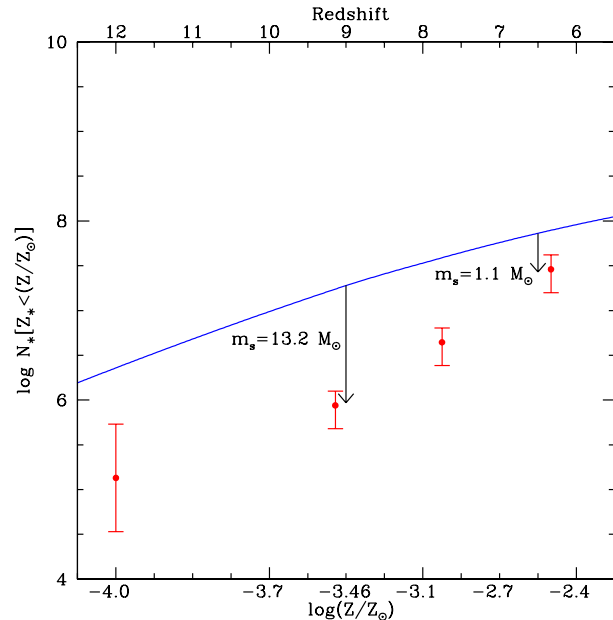


**Figure 5.** Average number of PopIII stars with metallicity lower than  $[Z/Z_\odot]$  expected in MW sized galaxies today, for a solar neighbourhood IMF (solid curve). The dots with error bars show the observations of Ryan & Norris (1991) and Beers *et al.* (1998), assuming an isothermal distribution for the stars in the halo (see text). The labeled arrows show the values of  $m_s$  required to reconcile model and data, at  $z = 6.5$  and  $z = 9.0$ .

(their NLTT sample) which is complete down to  $0.6M_\odot$  and  $V = 13.0$ , the same limit we use to sample our IMF. From the theoretical isochrones, this corresponds to a distance of 290 pc, which we take as the radius of the sample. In that sample 5 stars were found with  $[Z/Z_\odot] < -3.0$ . To obtain the total number of stars in the Galactic halo at this metallicity, we must introduce an assumption regarding the distribution of these stars.

If the PopIII stellar systems are disrupted while they are incorporated into the growing MW, their stars will today be found almost exclusively in the Galactic halo, while if the initial stellar systems form tight clusters, they might survive disruption and through dynamical friction end up in the galactic bulge. Which of these two processes dominates will depend on the mass ratio of the mergers through which the PopIII systems reach the MW. If these mass ratios are close to one, disruption will be important, while if they are accreted late into a fully formed MW PopIII objects might remain bound. From N-body simulations White & Springel (2000) have argued that most of the lowest metallicity stars in a present day galaxy will be found in the stellar halo, and not in the bulge. We therefore make the assumption that the lowest metallicity stars share the isothermal distribution of the dark halo, out to a distance of 100 kpc, representative of the total extent of the halo. The actual density profile of these objects might more closely resemble that of the old globular cluster population, having an  $R^{-3}$  profile. Fortunately, fixing the normalization point at the solar radius (8.5 kpc) yields total numbers which are largely independent of this change in the assumed profile, e.g. for



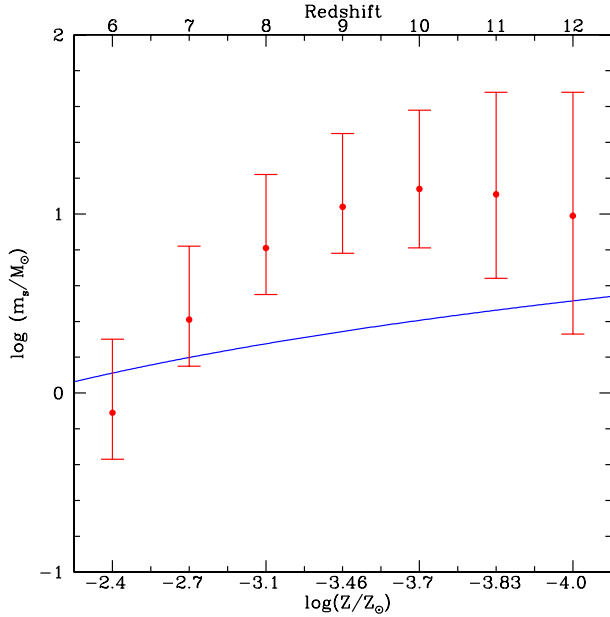


**Figure 6.** Inferred values of  $m_s$  as a function of redshift (points with error bars). The solid curve gives the redshift evolution of the Jeans mass of cold star forming clouds, identified with  $m_s$ , resulting from the temperature evolution of the cosmic microwave background (CMB).

core radii in the  $R^{-3}$  profile going from 0.2 to 2 kpc (a core radius must be introduced in the  $R^{-3}$  profile to avoid the central divergence), the total numbers of stars change by a factor 1.24 to 0.34, respectively, small compared to our error bars in figures 5 and 6. It is worth pointing out that the assumption of a particular density profile for the current low metallicity halo stars is not intrinsic to our results, but becomes necessary only for data comparison purposes.

Taking the Ryan & Norris (1991) data plus the hypothesis of an isothermal distribution discussed above, we derive the total number of stars with  $[Z/Z_\odot] < -3.0$  in the Galaxy as  $4.43 \times 10^6$ . To obtain numbers at other metallicities we use the relative metallicity distribution function of the more recent Beers *et al.* (1998) work, which combines several new samples. These observations are shown in Fig. 5 by the points with error bars, which reflect the uncertainties in the normalization.

The stellar halo might not extend as far out as 100 kpc, but some PopIII stars might be found in the bulge, so the interpretation of data used in Fig. 5 is probably a lower limit. On the other hand, given the uncertainties in the primordial IMF, our prediction is a strict upper limit.

It is clear that our results fall somewhat above the observational measurements, implying that our assumption of a constant  $m_s = 0.35M_\odot$ , essentially a present day solar neighbourhood IMF, is not valid. Reconciling our estimates with the observations requires not only the assumption of a higher  $m_s$  in the past, but throughout the redshift range studied, an increasing trend for this value. Note that our derived numbers of PopIII stars scale linearly with  $f_*$ .

Several authors, *e.g.* Larson (1998) have pointed out

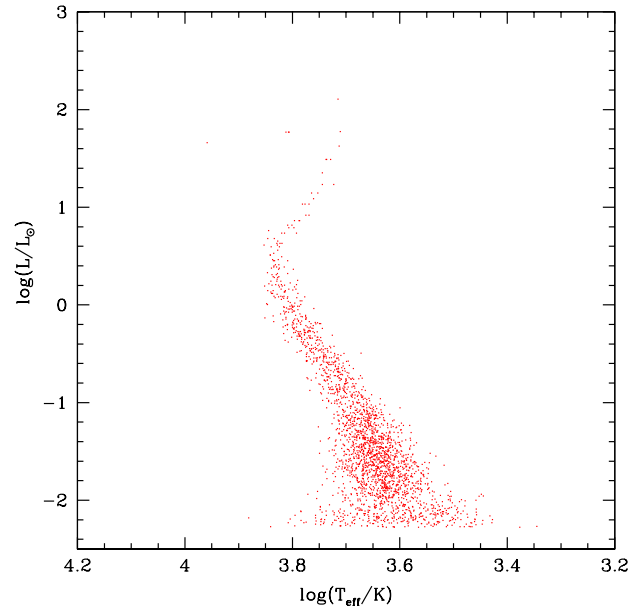


**Figure 7.** HR diagram for 2286 extremely low metallicity stars. Accurate isochrones for these stars are used to obtain good estimates of their present observational characteristics, which can be used to provide guidelines of their current photometrics and hence aid detection strategies.

that the increase of the CMB temperature with redshift alone, implies an increase in the Jeans mass for the star forming clouds, once one is beyond  $z = 2$ , where the CMB temperature equals the  $\approx 8$  K of cold star forming clouds. It has therefore been suggested that at high redshift the IMF should be increasingly weighted towards larger stellar masses. The labeled arrows in Fig. 5. show the values of  $m_s$  which we require at  $z = 6.5$  and  $z = 9.0$ , to match the observed points.

In Fig. 6 we show the values of  $m_s$  which we infer for the IMF of PopIII objects, by imposing that model and observations agree. The solid curve indicates the redshift evolution of the Jeans mass in star forming clouds, which we identify with  $m_s$ . Although for  $z < 9$  our results are consistent with the increase in  $m_s$  coming solely from that in the Jeans mass due to the CMB, the trend for  $6 < z < 9$  is clearly for a rise in  $m_s$  beyond what this effect can account for. In fact, as Larson (1998) points out, this is only the *minimum* increase to be expected, as other heating sources, *e.g.* massive stars themselves or a UV background, were likely to be present. Furthermore, a reduced opacity consistent with these low metal abundances would have the effect of skewing the IMF towards larger masses, thus operating in the same direction.

For  $z > 9$ , the values of the characteristic mass appear to stabilize around the value  $m_s = 10 - 15M_\odot$ , indicative of a very top heavy IMF at these early epochs, although the increase of our error bars makes determining trends in this redshift range harder.

Finally, Fig. 7 presents an HR diagram containing over 2000 stars, produced from the low metallicity stellar models used, convolved with errors appropriate to HST observations of halo stars (Gallart *et al.* 1999; Hernandez *et al.* 2000), for

$m_s = 5.0M_\odot$ . The inclusion of detailed atmosphere calculations and spatial information to yield detailed observational predictions will form part of a forthcoming paper.

## 5 SUMMARY

From our study we conclude that:

- If the standard hierarchical merger scenario is correct, in the MW one should not expect to find stars having metallicities lower than  $[Z/Z_\odot] = -4.3$ , consistent with current observational limits.
- We infer the IMF of PopIII stars to have been strongly weighted towards high masses, and increasingly more so in the range  $6 < z < 9$ , this levelling off at  $z \gtrsim 9$  at a characteristic mass scale  $m_s = 10 - 15M_\odot$ .
- Observational limits on the numbers and metallicity distribution of very low metallicity stars in the MW can place sharp restrictions on the IMF of the first stars. This can be achieved through detailed modelling of the full range of phenomena giving rise to such stars, of the type attempted here, thus necessarily establishing a connection with the underlying structure formation scenario.

## 6 ACKNOWLEDGMENTS

The authors wish to thank the referee, Volker Bromm, for his careful reading of the manuscript and helpful comments which improved the presentation of this paper, as well as Richard Larson for a detailed look at a first draft and Leo Girardi for making his new isochrones available electronically. This work was completed as one of us (AF) was a Visiting Professor at the Center for Computational Physics, Tsukuba University, whose support is gratefully acknowledged.

## REFERENCES

- Abel, T., Anninos, P., Norman, M. L. & Zhang, Y. 1998, ApJ, 508, 518
- Avila-Reese, V., Firmani, C., Klypin, A. & Kravtsov, A. V., 1999, MNRAS, 310, 527
- Beers, T. C., *et al.*, 1998, SSRv, 84, 139
- Binney, J., & Merrifield, M. 1998, Galactic Astronomy, (Princeton: UniPress)
- Bromm, V., Coppi, P. S. & Larson, R. B. 1999, ApJ, 527, L5
- Ciardi, B., Ferrara, A., Governato, F., & Jenkins, A., 2000, MNRAS 314, 611
- Dalcanton, J., Spergel, D. N., & Summers, F.J., 1997, ApJ, 482, 659
- Ferrara, A. 1998, ApJL, 499, 17
- Ferrara, A. 2000, preprint (astro-ph/0007179)
- Firmani, C., D'Onghia, E., Avila-Reese, V., Chincarini, G., Hernandez, X., 2000, MNRAS, 315, 29
- Flores R., Primack J. R., Blumenthal G. R., Faber S. M., 1993, ApJ, 412, 443
- Fryer, C. L., Woosley, S. E. & Heger, A., 2000, preprint (astro-ph/0007176)
- Fuller, T. M. & Couchman, H. M. P. 2000, preprint (astro-ph/0003079)
- Gallart C., Freedman W., Aparicio A., Bertelli G., Chiosi C., 1999, AJ, 118, 2245
- Girardi, L., Bressan, A., Bertelli, G., & Chiosi, C., 2000, A&AS 141, 371
- Gnedin, N. Y., & Ostriker, J. P., 1997, ApJ, 486, 581
- Haiman, Z. & Loeb, A. 1997, ApJ, 483, 21
- Hernandez, X., Gilmore, G., 1998, MNRAS, 294, 595
- Hernandez, X., Gilmore, G., Valls-Gabaud, D., 2000, MNRAS, in press
- Kashlinsky, A. & Rees, M. J. 1983, MNRAS, 205, 955
- Kulesha, A. S. & Lynden-Bell, D., 1992, MNRAS, 255, 105
- Lacey, C., & Cole, S., 1993, MNRAS, 262, 627
- Larson, R. B., 1998, MNRAS, 301, 569
- Machacek, M. E., Bryan, G. L. & Abel, T. 2000, preprint (astro-ph/0007198)
- Nakamura, T. & Umemura, M. 2000, preprint
- Nusser, A., & Sheth, R. K., 1999, MNRAS, 303, 179
- Omukai, K. & Nishi, R., 1999, ApJ, 518, 64
- Percival, W. & Miller, L., 1999, MNRAS, 309, 823
- Ripamonti, E., Haardt, F., Colpi, M. & Ferrara, A. 2000, in preparation
- Ryan, S. G., & Norris, J. E., 1991, AJ, 101, 1865
- Schneider, R., Ferrara, A., Ciardi, B., Ferrari, V. & Matarrese, S. 2000, MNRAS, in press (astro-ph/9909419)
- Steinmetz, M. & Navarro, J. 1999, ApJ, 513, 555
- Susa, H. & Umemura, M. 2000, ApJ, 537, 578
- Tegmark, M. *et al.* 1997, ApJ, 474, 1
- Umeda, H., Nomoto, K., & Nakamura, T. 2000, in The First Stars, ed. Weiss *et al.* (Berlin: Springer), 126
- White, S. D. M., & Springel, V. 2000, preprint (astro-ph/9911378)